

## ANALYSIS OF LEVITATION CHARACTERISTICS OF RADIAL-TYPE SUPERCONDUCTING MAGNETIC BEARINGS

**Hiromasa Fukuyama**

NSK Ltd., Fujisawa, Kanagawa, Japan, fukuyama-h@nsk.com

**Takeshi Takizawa**

NSK Ltd., Fujisawa, Kanagawa, Japan, takizawa-t@nsk.com

### ABSTRACT

In the design of large-scale flywheel, load capacity and bearing constants (i.e. spring and damping constants) should be accurately calculated. In this report, a newly developed analysis method for radial-type superconducting magnetic bearings (SMBs) composed of several couples of magnet rings and magnetic material spacers is described. The analysis method is based both on electromagnetic FEM of the magnetic field and the 2-Dimensional Bean Model for analysis of magnetization of oxide superconductors. To obtain accurate magnetization hysteresis that reflects the complex magnetic fields, a superconductor is meshed into cells. Then the electromagnetic force between the magnetic fields of magnets and the magnetization of the superconductor are calculated. Recently, computer programs which can calculate the axial load capacity and bearing constants of radial-type SMBs have been developed. Calculated results on axial load capacity showed good agreement with experimental results.

### INTRODUCTION

In response to increasing needs for electricity, surplus electricity during off-peak hours should be efficiently stored. There are several methods for storing electricity. Among them, the flywheel method is very useful. To store sufficient quantities of electricity, flywheels have to be large. The bearings for energy storage flywheels must have very low energy loss, so superconducting magnetic bearings (SMBs) are suitable for this purpose. [1][2] Particularly, radial-type SMBs are suitable for supporting the high loads and rotational speeds of energy storage flywheels. In the design of large flywheels, load capacity and bearing constants (i.e., spring and damping constants) should be accurately estimated.

YBaCuO superconductors fabricated by the so called melt-grown process (QMG)[3] or melt-powder-melt-growth(MPMG)[4] shows very strong magnetic force. These superconducting materials are suitable for the bearings of energy storage flywheel.

Concerning calculation method of levitation force of oxide superconductor, Sugiura [5] applied the magnetic vector potential (A) method to solve the Maxwell equations with a nonlinear J-E relation based on the critical state model. Tsuchimoto [6] analyzed numerically vertical levitation force in axial symmetric model using magnetic vector potential(A), and horizontal restoring force using current vector potential (T) method. There are several other calculation method has been published but there has not been reported about the calculation method of radial type SMBs. In this report, a newly developed analysis method for radial-type SMBs composed of superconductor and rotating magnetic structure is described. The analysis method is based both on electromagnetic FEM of the magnetic field and the 2-Dimensional Bean Model[7][8] for analysis of magnetization of oxide superconductors. The rotating magnetic structure is composed of several couples of magnetic rings and magnetic material spacers. The magnetic field generated by the magnetic structure is very complex, so to obtain accurate magnetization hysteresis of the superconductor, it is meshed into cells in the calculation. The magnetization hysteresis of each specific cell is affected by the changing magnetic fields caused by movement of the magnetic structure. Magnetization hysteresis is calculated using the 2-Dimensional Bean Model. Because the calculated magnetization of each specific cell is less than its actual magnetization, the effect of dividing the superconductor into cells must be corrected. After this is completed, the electromagnetic force between the magnetic fields caused by the magnetic structure and the magnetization



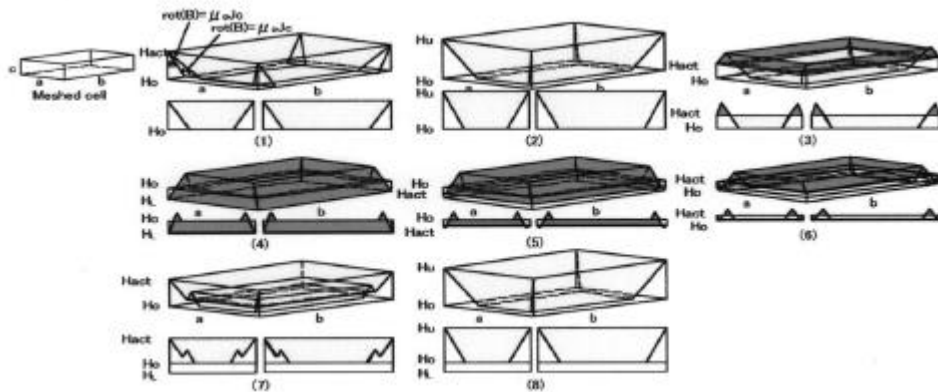


FIGURE 5: Magnetization Hysteresis by the 2-Dimensional Bean Model

application on each a and b side of the rectangular element. In the Bean Model when the acting magnetic field  $H_{act}$  on the element increases from the initial field cooling magnetic field  $H_b$ , the repulsive magnetization occurs and it is calculated as the volume of the solid which is enclosed within the lines whose gradients are  $\text{rot}(\mathbf{B}) = \mathbf{m} \times \mathbf{c}$ . The state (1) to (2) is the increasing external field. In this step, repulsive magnetization increases with increase in the external field. The state (2) is the nearest approach of the magnets to the superconductor. The process from (2) to (4) is the decreasing external field case. In this step, attractive magnetization is generated and increases canceling the previous repulsive magnetization. The state (4) is the farthest the magnetic rings get from the superconductor and the magnetization becomes only attractive. In (4) to (8), the increasing external field corresponds to the approach of the magnets to the superconductor. The state (8) is the same as (2). After (8), the process from (2) to (8) is repeated. Thus, repulsive and attractive magnetization is generated as hysteresis phenomena when magnets approach and remove from a superconductor.

**Automatic Calculation of Magnetization.** The magnetic field of radial-type SMBs is so complicated as shown in FIGURE 2 or FIGURE 3 that changes of magnetic field acting on each cell take varieties of patterns according to the movement of magnets. So it is needed to calculate magnetization automatically for any changing magnetic field. The new calculation method of automatic generation of magnetization is as follows.

The calculation method is divided into two cases. One is (a) when magnetization continues to increase or decrease, and the other is (b) when magnetization reverses from increasing to decreasing or from decreasing to increasing. FIGURE 6 shows these two cases.

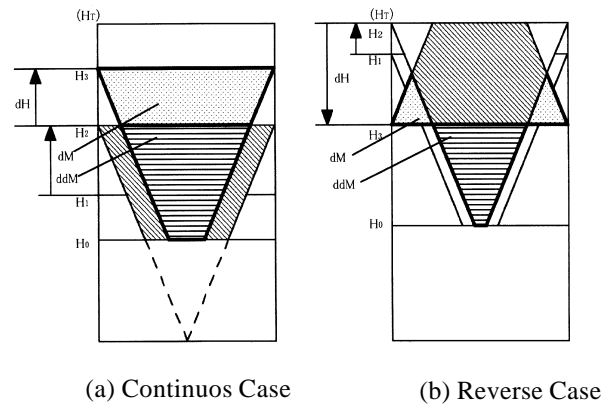


FIGURE 6: Auto-Creation of Magnetization

(a) Continuous case: In FIGURE 6, magnetic field increases continuously like from  $H_1$  to  $H_2$  to  $H_3$ .

Magnetization at  $H_3 = dM + ddM$

Here,  $dM$  is the generated magnetization when magnetic field changed from  $H_2$  to  $H_3$  and  $ddM$  is the magnetization that remains after deleting the diagonally lined sections in FIGURE 6 (a).

(b) Reverse case: In FIGURE 6, magnetic field reverses from  $H_1$  to  $H_2$  to  $H_3$ .

Magnetization at  $H_3 = dM + ddM$

Here, the pole sign of  $dM$  is opposite to  $ddM$ .

$dM$  : the magnetization that remains after deleting the diagonally lined section in FIGURE 6 (b) when magnetic field changed from  $H_2$  to  $H_3$ .

$ddM$  : the residual magnetization which is deleted the magnetization that is generated when magnetic field changed from  $H_2$  to  $H_3$  from the magnetization that had possessed at  $H_2$ .

**Correction of the effect of Meshing.** In the calculation the effect of meshing has to be corrected. FIGURE 7 shows the magnetization of a single crystal by the 1-Dimensional Bean model. The crystal is large enough for the acting magnetic field to not be uniform as shown by broad line in FIGURE 7. In FIGURE 7, the crystal is

divided into 4 parts and in each part the average acting magnetic field ( $H_{a1}, H_{a2}, H_{a3}, H_{a4}$ ) is different from each other. In the figure, the whole average acting magnetic field of the entire crystal is also represented as  $H_a$ . Magnetization calculated in the divided parts by Bean model is represented by hatched triangle. This magnetization is not correct. It is corrected as follows.

Accurate magnetization generated in part 1 where average magnetic field  $H_{a1}$  is acting can be obtained by widening that part size ( $W/4$ ) to whole size ( $W$ ), acting  $H_{a1}$  on the whole size and dividing the obtained magnetization by 4. The same procedure is used in the other parts. Magnetization of the divided parts by this means is shown in FIGURE 3. The total magnetization of the whole crystal should be the sum of the magnetization of the 4 parts.

In the 2-Dimensional Bean model, the same procedure is used both in length and in width. That is as follows. When a superconductor ring is meshed into cells, a single crystal is meshed by  $m$  in length and meshed by  $n$  in width as one group. In the calculation of the magnetization of the meshed cell, the length of meshed cell is multiplied by  $m$  and the width is multiplied by  $n$ . The calculated value is divided by ( $m \cdot n$ ) and then it becomes real value of the meshed cell. Hysteresis of magnetization of each cell takes various pattern due to complex magnetic field. FIGURE 8 shows several hysteresis of magnetization in cells.

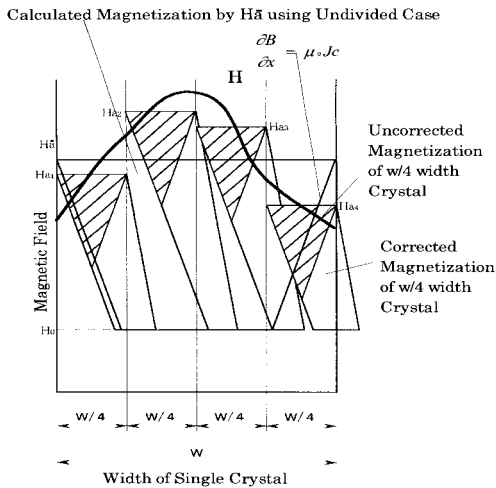


FIGURE 7: Correction of Meshing

**Levitation Force Analysis.** Levitation force of SMBs can be obtained by electromagnetic force between magnetization in each cell and magnetic field. The levitation force  $f$  of a cell whose volume is  $dv$  can be calculated as follow

$$f = m \bullet \nabla B dv \tag{1}$$

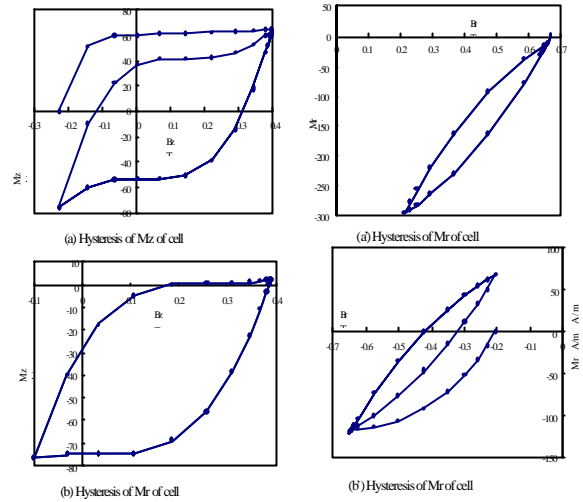


FIGURE 8: Magnetization Hysteresis of cells

here,  $m$  is magnetization, and  $B$  is magnetic flux density.

The levitation force  $F$  of the whole superconductor is

$$F = \int m \bullet \nabla B dv \tag{2}$$

Equation (2) is represented as eq.(3)

The levitation force in axial direction is  $F_z$ .  $F_z$  of radial-type SMBs can be treated as axial symmetric problem and  $x$  is replaced as  $r$ .

And  $F_z$  is represented as eq.(4).

$$\left. \begin{aligned} F_x &= \sum (m_x \frac{\mathcal{B}_x}{\mathcal{K}} + m_y \frac{\mathcal{B}_x}{\mathcal{K}} + m_z \frac{\mathcal{B}_x}{\mathcal{K}}) dv \\ F_y &= \sum (m_x \frac{\mathcal{B}_y}{\mathcal{K}} + m_y \frac{\mathcal{B}_y}{\mathcal{K}} + m_z \frac{\mathcal{B}_y}{\mathcal{K}}) dv \\ F_z &= \sum (m_x \frac{\mathcal{B}_z}{\mathcal{K}} + m_y \frac{\mathcal{B}_z}{\mathcal{K}} + m_z \frac{\mathcal{B}_z}{\mathcal{K}}) dv \end{aligned} \right\} \tag{3}$$

$$F_z = \sum (Mr \frac{\mathcal{B}_z}{\mathcal{K}} + Mz \frac{\mathcal{B}_z}{\mathcal{K}}) \nabla n \tag{4}$$

$Mr, Mz$  can be obtained from  $Br, Bz$  and

$\frac{\mathcal{B}_z}{\mathcal{K}}, \frac{\mathcal{B}_z}{\mathcal{K}}$  can be obtained from  $Bz$ .

The levitation force hysteresis is obtained by equation (1) using the hysteresis of  $m$ . Examples of levitation force hysteresis of cells are shown in FIGURE 9. The levitation force hysteresis of the whole superconductor is obtained by equation (2) or (3). In the case of FIGURE

2,  $z - Bz, \frac{\mathcal{B}_z}{\mathcal{K}}, \frac{\mathcal{B}_z}{\mathcal{K}}$  are shown in FIGURE 9.

Levitation force hysteresis of cell (1,13) and (1,30) are shown in FIGURE 10. Levitation force hysteresis of the whole superconductor can be obtained by summing up the levitation force hysteresis of each cell.

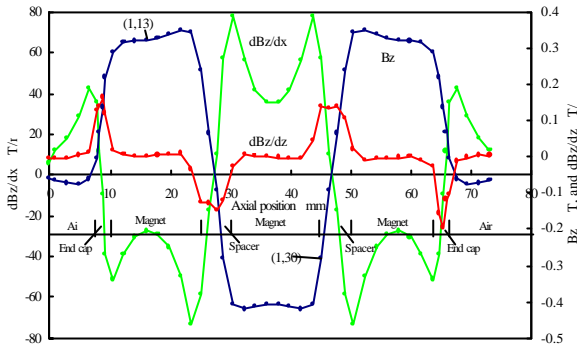


FIGURE 9:  $z - B_z, \frac{\partial B_z}{\partial r}, \frac{\partial B_z}{\partial z}$

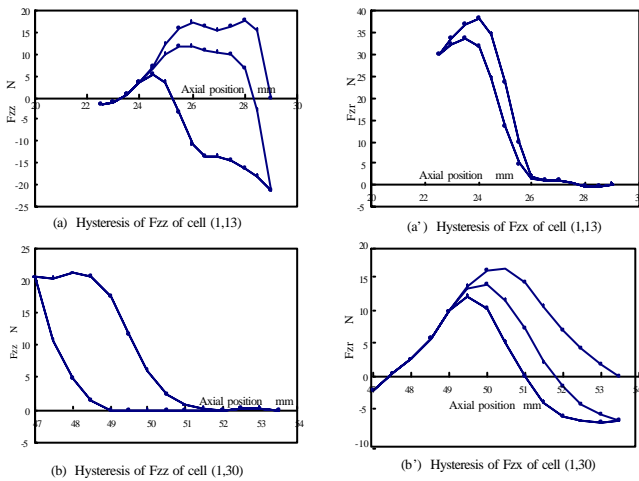


FIGURE 10: Hysteresis of  $F_{zz}, F_{zx}$  of cell (1,13) and (1,30)

**EXPERIMENT AND COMPARISON**  
**Experiment**

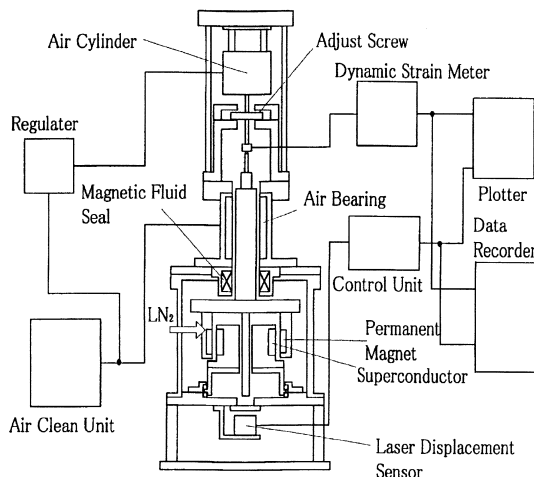


FIGURE 11: Experimental Equipment

To investigate the accuracy of the calculation calculated results were compared with experimental results. The experimental equipment is shown in FIGURE 11. The tested bearing size is shown in FIGURE 11. The tested bearing size is shown in FIGURE 1.

The tested materials of the magnets were Pr and NdFeBo. The superconductor ring was composed with 6 or 8 arc shaped bulk superconductor. In the calculation critical current density of the superconductor was set as  $1.5e7 (A/m^2)$ .

**Comparison**

**Comparison 1:** Experimented levitation force hysteresis of the case of 6 divided superconductor-Pr magnet is shown in FIGURE12. The calculated results is shown in FIGURE 13 and the calculated result shows good agreement with the experimented result.

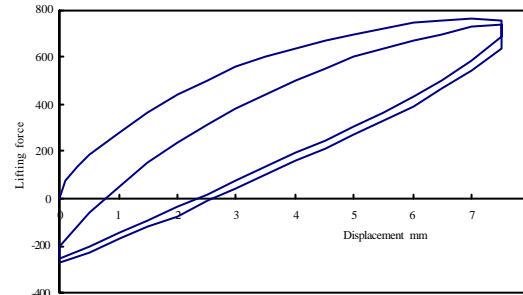


FIGURE 12: Levitation Characteristics of Pr-Magnet-6-Divided SC

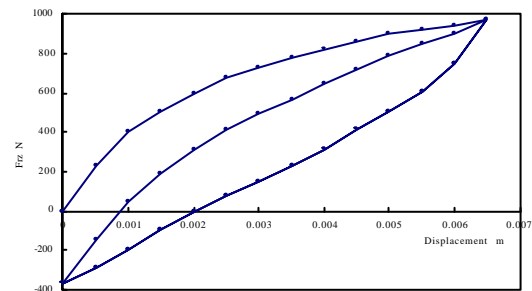


FIGURE 13: Calculated Result of FIGURE 12

**Comparison 2:** Experiments were executed in the following cases according to number of dividing superconductor and materials of magnets.

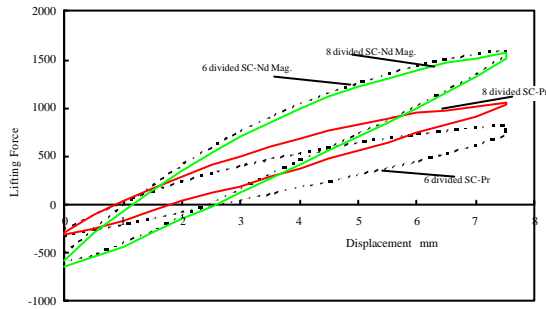
- (a) 6 divided superconductor and Pr magnet
- (b) 8 divided superconductor and Pr magnet
- (c) 6 divided superconductor and Nd magnet
- (d) 8 divided superconductor and Nd magnet

FIGURE 14 shows the experimental results. FIGURE 15 shows calculated results.

In the experiments, Nd magnet types had larger characteristics than Pr magnet types because of their higher magnetic fields.

In the case of Nd magnets, 6 divided Sc-Nd magnet showed a little larger characteristics but the difference was small between them. In the case of Pr magnet, 8divided SC type showed larger characteristics than 6 divided SC type.

On the other hand, the calculation gave results that 6 dived SC always shows larger characteristics than 8 divided SC because 6 divided SC has larger bulk size than 8 divided SC. The difference between experiment and calculation comes from the fact that experimental results are effected by the state of fabrication of SMBs. Anyway comparing the calculated results with the experimental results the calculated results gave almost the same order results in value.



**FIGURE 14:** Experimental Results of 6- and 8-Divided SC-Pr and Nd Magnets

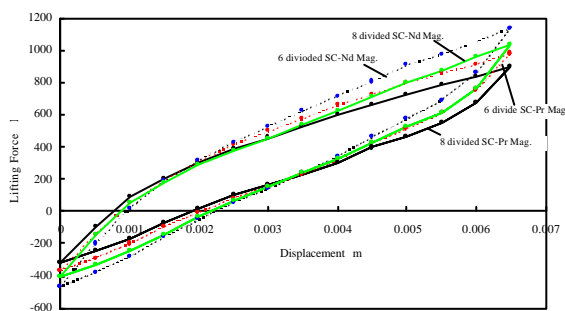


**FIGURE 15:** Calculated Results of FIGURE 14

## CONCLUSION

(1) The calculated results on levitation characteristics showed good agreement with the experimental results. This calculation method is effective for calculating the axial characteristics of radial-type SMBs.

(2) An analysis method has been established in which

the magnetic field of magnets is calculated by electromagnetic FEM and the superconductor is meshed into cells for calculation. The magnetization in each cell is calculated using the 2-Dimensional Bean Model. Levitation force of SMBs can be obtained by summing up the electromagnetic force between the magnetization in each cell and magnetic field.

(3) A method has been developed for auto-generating calculation of magnetization in a meshed cell of a superconductor under a complex magnetic field.

## ACKNOWLEDGEMENTS

The authors are pleased to acknowledge that this work was carried out under the contract of the project "The Research and Development of Electric Energy Storage by Flywheel using High Temperature Superconductor" by New Energy and Industrial Technology Development Organization (NEDO).

## REFERENCE

1. Higasa H., Ishikawa F. et al.. Experiment of a 100Wh-Class Power Storage System using High-Tc Superconducting Magnetic Bearing, *Adv. in Superconductivity 4th*: 1249-1252, 1994.
2. Bornemann H.J. et al.. A FLYWHEEL FOR ENERGY STORAGE WITH FRICTIONLESS HIGH TEMPERATURE SUPERCONDUCTOR BEARINGS, 4th Int. Sym. On Magnetic Bearings, Aug. 1994.
3. Morita M. et al., Processing and properties of QMG materials, *Physica C (235-240)*:209-212, 1994
4. Murakami M. et al., Large levitation force due to flux pinning YBaCuO superconductors fabricated by Melt-Powder-Melt-Growth Process, *Jpn. J. Appl. Phys.* 29, L1991, 1990
5. Sugiura T., Hashizume H. and Miya K., Numerical electromagnetic field analysis of oxide superconductors, *Int. J. Appl. Electromagn. Mater.* 2:183, 1991
6. Tsuchimoto M., Takeuchi H. and Honma. T., Numerical Analysis of Levitation Force on a High Tc Superconductor for Magnetic Field Configuration, *T. IEE Jpn.* 114-D,7/8:741, 1994.
7. Murakami, M., *Melt Processed High-temperature Superconductors*, World Scientific Publishing, 1992
8. Fukuyama H., Takizawa T., Analysis of the levitation characteristics of superconducting bearings, *Proc. 6th Int. Symp. on Magnetic Bearings*, Technomic Publishing Co., Boston, 1998.